FIBRES & TEXTILES in Eastern Europe

sciendo

FIBRES & TEXTILES in Eastern Europe

Research Article • DOI: 10.2478/ftee-2022-0022 FTEE • 151(3) • 2022 • 46–56

Coefficients for Assessing the Visibility of Materials Used in Anti-Smog Face Masks

Agnieszka Brochocka[1]*, Grzegorz Owczarek[1], Joanna Szkudlarek[1]

[1] *Central Institute for Labour Protection, National Research Institute, Department of Personal Protective Equipment, 00-701 Warsaw, Poland*
** Corresponding author. E-mail: agbro@ciop.lodz.pl*

Abstract
The application of phosphorescence for the modification of face mask materials is motivated by the need to appreciably increase their visibility while using graphical elements with a relatively small area. Phosphorescent dyes absorb part of the visible spectrum while emitting radiation at wavelengths that are longer than the absorbed ones. Thus, a phosphorescent substance can emit light even if it is not being illuminated at a given time (but was before). This paper describes studies of the optical properties based on parameters such as the reflectance coefficient, chromaticity coordinates, as well as luminance measured from digital images for two models of smog-protective face half-masks differing in terms of their inner layer with filtration properties and outer printed layer. The external surface of one mask type is printed with a phosphorescent solid star pattern, while the other with a phosphorescent open star pattern. The influence of the inner filter layer was assessed in correlation with the colour of the outer layer and the type of printing. Moreover, the phenomenon of phosphorescence was identified. The study resulted in developing a material with properties providing better visibility under defined use conditions.

Keywords
spunbond nonwoven, phosphorescent material, face half-mask, coefficient of reflectance, chromaticity coordinates, luminance.

1. Introduction

Visibility is a very broad concept in terms of its definition as well as material properties, observation conditions, and the nature of human eyesight. There is a major difference between object visibility, which is a property of materials independent of the circumstances of observation, and visibility conditions, which determine our ability to see things. Anti-smog face masks are naturally used under low visibility conditions, and so it is necessary to increase their object visibility, which mostly depends on optical properties, although other factors, such as motion, may also be at play. The fact that moving objects are more readily perceptible is attributable to the physiology of human vision.

In the case of personal protective equipment (PPE), optical properties are mostly associated with materials reflecting, scattering, and transmitting optical radiation in the visible (VIS), ultraviolet (UV), and infrared (IR) ranges, which are collectively known as optical materials. Their applications in PPE include eye protection elements and high visibility devices (background and reflective elements). The optical materials used for eye protection mostly involve polymers and mineral glass [2]. The background materials in clothing usually exhibit vivid colors (mostly yellow or orange). In turn, reflective materials are made of micro-lenses or micro-prisms [3].

Regardless of their application, transparent materials are characterised by such parameters as transmission, absorption, and reflection/scattering of UV-VIS-IR radiation. The transmission/absorption spectral characteristics of transparent optical materials determine their colour. Similarly to transparent materials, textile fabrics also reflect/scatter UV-VIS-IR light. In the case of selected textile materials (e.g., those used for blocking visible light), the parameters describing their optical properties are tested and analysed in great detail [3].

Most textile materials used in PPE are completely or mostly opaque to VIS due to their functions as they are not intended to be translucent. In addition to their basic barrier functions, such as the protection of the human body against external factors including heat/cold, rain, moisture, and UV radiation, textile materials may also be designed to reflect VIS to improve the user's visibility. Colour, retroreflective properties, and sometimes also phosphorescence, influence the visibility of textile materials under given conditions (day/night, varying weather, etc.).

The basic parameters describing the visibility properties of textile materials are as follows [4]:
– the luminance coefficient,
– chromaticity coordinates.

The highest levels of user visibility are provided by PPE, such as warning clothing (for both occupational and casual use) and reflective accessories. Pursuant to Regulation (EU) 2016/425 of the European Parliament and of the Council [5], such devices are classified as category II PPE, and therefore they must meet the essential requirements concerning, amongst others, photometric properties for devices used to ensure the wearer conspicuity under given conditions.

Following trends in clothing design, it can be seen that the visibility aspect is increasingly emphasised not only in the case of protective clothing but also in non-occupational casual apparel. Reflective elements are now widely used in jackets,

trousers, headwear, and footwear. Such elements may be incorporated into textile materials using different methods. A novel technology of high-quality in situ phosphorescent printing with a potential for continuous roll-to-roll industrial production was proposed by Zhang et al. [6]. Phosphorescent moieties were covalently connected to a polyethylene-polypropylene nonwoven. The resulting material emitted bright blue light with a high quantum yield (~83.35%), which could be attributed to aggregation-induced emission. The high-resolution printing technology enabled the production of a wide range of phosphorescent patterns and shapes on nonwovens. The versatility of the method was demonstrated by producing phosphorescent materials with different polymeric matrices, such as Nylon 66 and a polyethylene terephthalate membrane [6].

In another paper [7], water-soluble phosphorescent flavin mononucleotide (FMN) bio-molecules derived from vitamin B2 were used to produce a glow-in-the-dark photoluminescent polyester emitting yellow-green light. The paper analysed different ways of incorporating the phosphorescent substance into the nonwoven, such as screen printing and coating with gelatin, sodium alginate, and water-soluble polyacrylate while also activating the nonwoven with air-atmospheric plasma treatment for improved spreading. The authors reported gelatin to be an ideal polymeric coating and binder for observing the phosphorescent properties of FMN in printed patterns. The deposition of such a coating on a PET nonwoven subjected to plasma treatment enhanced the resistance of the phosphorescent product to washing under harsh chemical conditions. In turn, the authors of [8] imparted phosphorescent properties to a nonwoven made of polyethylene and polypropylene fibers induced with preliminary irradiation with an electron beam. The fibers revealed intensive phosphorescence, a high quantum yield (>90%) and excellent stability after washing under harsh conditions. Moreover, the colour and intensity of the phosphorescence, quantum yield as well as phosphorescence duration may be controlled using aggregation-induced phosphorescence quenching. Due to the aggregation-caused quenching (ACQ) effect, aggregates have limited applicability in layers emitting light. On the other hand, phosphorescent fabrics prepared in this way may effectively distinguish between monocyclic aromatic hydrocarbons as a result of adsorption-induced phosphorescence changes. Therefore, such nonwovens may be used as chemical sensors, photoelectric materials, as well as for decorative purposes.

It should be noted that wearer visibility can also be increased by face masks, which may be very useful for at least two reasons. First of all, face masks can protect the respiratory system against smog pollution, which in Poland occurs mostly in the autumn and winter [9]. Secondly, due to the global pandemic of SARS-CoV-2, face mask use has become commonplace [10–12]. Given the current epidemiological data, there is no indication that the widespread obligation to cover one's mouth and nose with face masks will be lifted any time soon [13].

For a face mask to be user friendly, it must offer a high level of comfort provided by low airflow resistance. Thus, phosphorescent marking is suitable for facemasks as it substantially enhances visibility while taking up a relatively small area. Phosphorescent dyes absorb wavelengths from a certain part of the visible light spectrum, re-emitting wavelengths that are longer than the absorbed ones. Importantly, phosphorescent substances may emit light even if they are not currently illuminated, but were before.

The objective of the study was to assess the visibility of the material with a phosphorescent pattern of a half-mask protecting against smog applied using the available laboratory methods.

2. Materials

The study involved two samples of materials intended for anti-smog face masks. The samples were made of a non-woven printed with a yellow-green phosphorescent dye and differed in terms of the print pattern and background colour. Sample 1 was blue and featured an open star pattern, while sample 2 was white and featured a solid star pattern (see Figure 1).

The nonwovens shown in Figure 1 were used as the outer layers in the anti-smog filtering-absorbent face mask models presented in Figure 2. The outer layers featured phosphorescent patterns made by means of screen printing: open and solid stars. It should be noted that screen-printed patterns cannot be arranged too densely on the surface as the dye filling the voids between fibers, can increase breathing resistance, which adversely affects user comfort. Air flow resistance for printed and non-printed material is presented in Table 1.

The half-mask models presented in Figure 2 consisted of the following layers:

Model A
- blue spunbond outer layer printed with a phosphorescent pattern in the form of open stars, with a surface density of 86 g/m^2,
- middle filtering-absorbent layer with a surface density of 150 g/m^2,
- inner spunbond layer, with a surface density of 50 g/m^2.

Model B
- white spunbond outer layer with a printed phosphorescent pattern in the form of solid stars, with a surface density of 84 g/m^2,
- middle filtering-absorbent layer, with a surface density of 150 g/m^2,
- inner spunbond layer, with a surface density of 50 g/m^2.

The spun-bond nonwovens with a pattern printed with phosphorescent ink constituting the external layer of the filtering half-mask had the same surface weight. The materials differed only in colour. In order to determine how the colour of the material affects its visibility, the optical properties were determined.

The phosphorescent effects on the outer layers of the two half-mask models are presented in Figure 3.

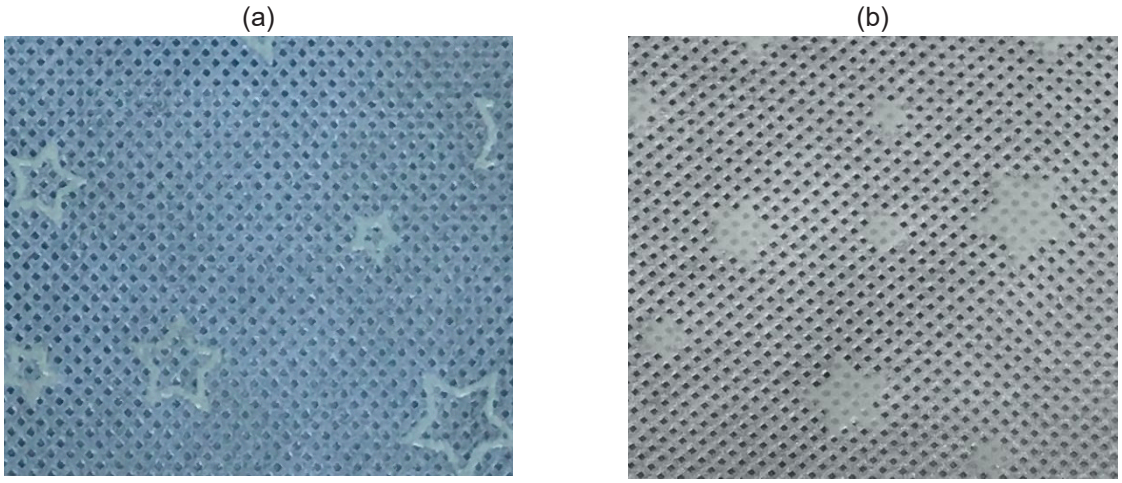

Fig. 1. Materials studied: (a) – sample 1, blue nonwoven printed with an open star pattern, (b) – sample 2, white nonwoven printed with a solid star pattern

Fig. 2. Models of anti-smog half-masks: (a) – model A – sample 1, the outer layer printed with a phosphorescent open star pattern, (b) – model B – sample 2, the outer layer printed with a phosphorescent solid star pattern

No.	Type of nonwoven fabric	Air flow resistance, Pa
1	Nonwoven fabric printed with an open star pattern	23,5
2	Nonwoven fabric printed with a solid star pattern	28,7
3	Nonwoven fabric without printing	21,6

Table 1. Air flow resistance comparison for printed and non-printed material

3. Parameters for visibility evaluation and methods for their determination

Measurements of the samples with phosphorescent printed patterns described in the previous section included the reflectance coefficient, chromaticity coordinates, and luminance determined from digital images.

3.1. Determination of the reflectance coefficient and chromaticity coordinates

The reflectance (brightness) coefficient and chromaticity coordinates (colour measurements) are used for assessing high-visibility materials, including those incorporating phosphorescent dyes, used in the production of warning clothing which provides wearer conspicuity under conditions of insufficient lighting, e.g., at dusk.

Colour measurements using a reflectometer involve measuring the ratio of reflected light to incident light in the 400–700 nm range. According to publications by the International Commission on Illumination (CIE), the light beam reflected off an object (usually a vividly coloured sample) may be expressed in terms of its

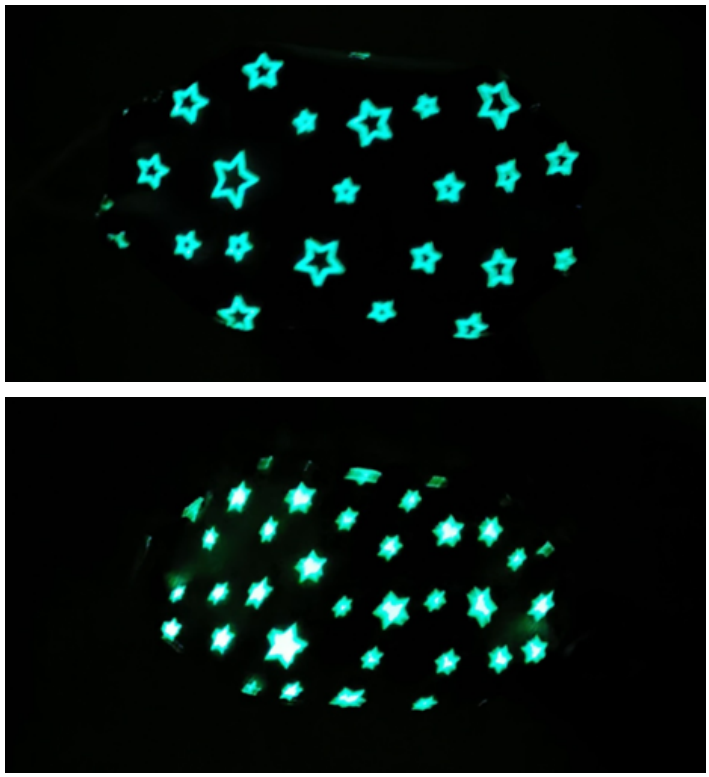

Fig. 3. Studied half-mask models with phosphorescent patterns in a dark room: (a) model A - with an open star pattern, (b) model B - with a solid star pattern

Fig. 4. MiniScan XE Plus reflectometer (USA) used for determining the reflectance coefficient and chromaticity coordinates

trichromatic components: X, Y, and Z. These components may be calculated using mathematical equations based on measurements of re-emission from the sample. Subsequently, one can use tables with data on the illuminant $s(\lambda)$ and the observer $x(\lambda)$, $y(\lambda)$, $z(\lambda)$ to produce a re-emission curve expressing the relationship between the reflection coefficient R and wavelength $f(\lambda) = R$. It should be borne in mind that the results are significantly affected by measurement geometry, i.e., the angles of incidence and reflection, the light source (illuminant D65, A), and parameters of the optical analyser (monochromator), that is, the observer (normal observer 2º or 10º).

According to the requirements of the standard PN EN 20471:2013-07/A1 [14], colour should be measured pursuant to the procedures stipulated by the International Commission on Illumination (CIE) [15] using a polychromatic light source (illuminant D65), a 45/0 geometry (the angle of reflection to the angle of incidence), and a normal observer. This produces the chromaticity coordinates x, y and Y and the luminance coefficient β, which is computed from Equation 1 on the basis of the coordinate values obtained. The colour coordinates x and y express hue and saturation, while Y stands for brightness, ranging from 0 for black to 100 for white.

$$\beta = 100/Y \quad (1)$$

The requirements contained in PN-EN 20471:2013-07/A1 concern high visibility materials for occupational use which are yellow ($\beta < 0.75$) or orange ($\beta < 0.40$).

Figure 4 shows a photograph of the MiniScan XE Plus reflectometer (USA) used for determining the reflectance coefficient and chromaticity coordinates in the preliminary studies of face mask materials. During the measurements, the materials were placed on a black metal plate and a white metal plate (reference plates in reflectance studies), as well as grey and white nonwovens. Prior to the measurements, the samples were conditioned for at least 60 min in a room illuminated with artificial light (fluorescent lamps). The intensity of incident light was approx. 500 lx.

3.2. Determination of luminance from digital images

The potential visibility of face mask materials with phosphorescent print patterns was also evaluated using an image analysis method which compared RGB values (ranging from 0 to 250) obtained for the sample printed surface following irradiation with artificial or natural light and the same printed surface conditioned in complete darkness (non-irradiated). RGB (red, green, blue) is a widely used colour space model which follows the way the human eye perceives colours.

A comparison of RGB values in photographic images of irradiated and non-irradiated samples makes it possible to evaluate the luminance of the materials studied. The higher the RGB values of an image (given the same photographic conditions), the greater the potential visibility of the material. The sample conditioning parameters can be set to arbitrary values. The main idea of the method proposed is to determine RGB in images representing the outer layer of the samples produced. For the purpose of comparison, it is necessary to maintain the same sample lighting level when taking photographs and the same camera settings (exposure time, aperture, distance between the camera matrix and the sample surface).

4. Results and discussion

4.1. Determination of the luminance coefficient and chromaticity coordinates

The method proposed was used to assess the influence of the colour of the inner filtering layer (white/gray) in correlation with that of the outer layer (blue/white) and the type of printed pattern. Tables 2–5 show the luminance coefficient β and chromaticity coordinates (both expressed in relative units) for sample 1 for all the aforementioned material-background configurations.

Given that the material studied featured a luminescent pattern, the most reliable indicator for determining differences in its visibility was the luminance coefficient β. The reflectance of the sample placed on a white reference background was higher by 44% as compared to the same sample on a black background. When the sample was placed on a white nonwoven, it also led to a small increase in β values, from 0.402 (white background) to 0.420 (white nonwoven). The lowest luminance coefficient was obtained for a black reference plate (0.227), and the highest – for the white nonwoven (0.420). The reflectance coefficient of sample 1 placed on a grey nonwoven was slightly higher than that for the same sample placed on

Measurement No.	*Y*	*x*	*y*	*β*
1	23.460	0.279	0.305	0.235
2	22.600	0.277	0.301	0.226
3	22.180	0.279	0.304	0.222
4	22.810	0.278	0.303	0.228
5	22.330	0.278	0.303	0.223
6	22.950	0.278	0.304	0.230
7	22.400	0.279	0.304	0.224
8	23.320	0.280	0.306	0.233
9	22.430	0.279	0.304	0.224
10	22.520	0.277	0.302	0.225
Mean	**22.700**	**0.278**	**0.303**	**0.227**
Standard deviation	**0.428**	**0.001**	**0.001**	**0.004**

Table 2. Luminance coefficient β and chromaticity coordinates for sample 1 on a black reference plate

Measurement No.	*Y*	*x*	*y*	*β*
1	41.900	0.270	0.299	0.419
2	39.480	0.264	0.293	0.395
3	41.410	0.270	0.298	0.414
4	42.510	0.272	0.301	0.425
5	38.220	0.267	0.298	0.382
6	40.630	0.267	0.295	0.406
7	39.730	0.267	0.295	0.397
8	39.810	0.272	0.298	0.398
9	39.430	0.268	0.297	0.394
10	38.880	0.267	0.295	0.389
Mean	**40.200**	**0.268**	**0.297**	**0.402**
Standard deviation	**1.375**	**0.003**	**0.002**	**0.014**

Table 3. Luminance coefficient β and chromaticity coordinates for sample 1 on a white reference plate

Measurement No.	*Y*	*x*	*y*	*β*
1	40.520	0.266	0.294	0.405
2	42.080	0.267	0.294	0.421
3	41.390	0.265	0.293	0.414
4	41.750	0.266	0.294	0.418
5	43.330	0.268	0.296	0.433
6	41.900	0.267	0.294	0.419
7	42.840	0.272	0.294	0.428
8	41.600	0.267	0.296	0.416
9	42.430	0.268	0.295	0.424
10	42.490	0.270	0.298	0.425
Mean	**42.033**	**0.268**	**0.295**	**0.420**
Standard deviation	**0.795**	**0.002**	**0.001**	**0.008**

Table 4. Luminance coefficient β and chromaticity coordinates for sample 1 on a white nonwoven

Measurement No.	*Y*	*x*	*y*	*β*
1	22.870	0.278	0.303	0.229
2	24.230	0.280	0.306	0.242
3	24.350	0.279	0.304	0.244
4	23.080	0.278	0.303	0.231
5	23.340	0.280	0.305	0.233
6	23.780	0.279	0.304	0.238
7	23.120	0.279	0.303	0.231
8	23.750	0.279	0.304	0.238
9	23.920	0.278	0.303	0.239
10	23.190	0.277	0.302	0.232
Mean	**23.563**	**0.279**	**0.304**	**0.236**
Standard deviation	**0.513**	**0.001**	**0.001**	**0.005**

Table 5. Luminance coefficient β and chromaticity coordinates for sample 1 on a grey nonwoven

Measurement No.	Y	x	y	ß
1	39.280	0.313	0.330	0.393
2	37.500	0.312	0.328	0.375
3	37.790	0.313	0.330	0.378
4	37.530	0.312	0.328	0.375
5	40.180	0.313	0.330	0.402
6	39.170	0.313	0.330	0.392
7	40.040	0.313	0.330	0.400
8	39.080	0.312	0.329	0.391
9	40.960	0.313	0.330	0.410
10	40.820	0.313	0.330	0.408
Mean	**39.235**	**0.313**	**0.329**	**0.392**
Standard deviation	**1.294**	**0.000**	**0.001**	**0.013**

Table 6. Luminance coefficient β and chromaticity coordinates for sample 2 on a black reference plate

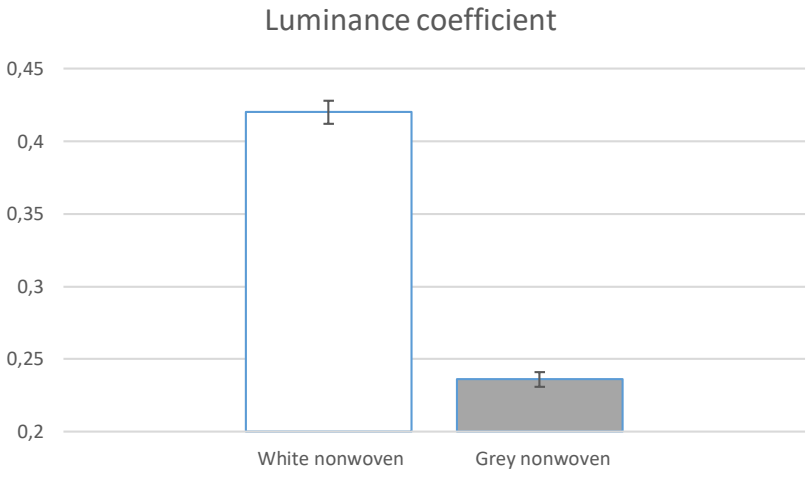

Fig. 5. Luminance coefficient β for samples placed on white and grey nonwovens

a black reference background (0.236 vs. 0.227).

Figure 5 shows a comparison of the mean luminance coefficient for the sample placed on white and grey nonwovens.

Luminance coefficients for the sample placed on white and grey nonwovens are 0.420 ± 0.008 and 0.236 ± 0.005, respectively, which indicates better visibility in the case of using a white nonwoven. Therefore, measurements of the luminance coefficient and chromaticity coordinates for sample 2 excluded the grey background. The ratio of reflected to incident light for the white nonwoven is significantly greater than for the grey nonwoven.

Tables 6–8 show luminance coefficients and chromaticity coordinates for sample 2 for all the aforementioned sample-background configurations.

The lowest luminance coefficient for sample 2 (with a pattern of solid stars on a white background) was obtained for the sample placed on a black background (0.392±0.013), and the highest for that placed on a white nonwoven – 0.849±0.008.

Figure 6 shows a comparison of mean luminance coefficients for samples 1 and 2 placed on a white nonwoven.

Reflectance coefficients for samples 1 and 2 on a white nonwoven were 0.420±0.008 and 0.849±0.008, respectively, which means that sample 2 can potentially provide better visibility.

4.2. Luminance determination from digital images

The method of luminance determination from digital images proposed was used to evaluate the phosphorescence phenomenon of the outer printed layer, A preliminary study was conducted to compare RGB values for the two material samples described in the previous section: sample 1 - with an open star print pattern

Measurement No.	Y	x	y	ß
1	84.250	0.314	0.333	0.843
2	84.510	0.315	0.335	0.845
3	84.060	0.313	0.332	0.841
4	84.470	0.315	0.335	0.845
5	83.270	0.314	0.332	0.833
6	83.510	0.313	0.331	0.835
7	83.960	0.314	0.333	0.840
8	82.490	0.314	0.33`9	0.825
9	83.970	0.313	0.331	0.840
10	83.890	0.314	0.332	0.839
Mean	**83.838**	**0.314**	**0.333**	**0.838**
Standard deviation	**0.610**	**0.001**	**0.001**	**0.006**

Table 7. Luminance coefficient β and chromaticity coordinates for sample 2 on a white reference plate

Measurement No.	Y	x	y	ß
1	85.060	0.314	0.333	0.851
2	85.060	0.315	0.335	0.851
3	84.490	0.314	0.332	0.845
4	84.300	0.314	0.333	0.843
5	85.960	0.314	0.333	0.860
6	85.830	0.314	0.332	0.858
7	85.580	0.314	0.332	0.856
8	83.750	0.315	0.334	0.838
9	84.760	0.315	0.333	0.848
10	84.030	0.314	0.332	0.840
Mean	**84.882**	**0.314**	**0.333**	**0.849**
Standard deviation	**0.755**	**0.001**	**0.001**	**0.008**

Table 8. Luminance coefficient β and chromaticity coordinates for sample 2 on a white nonwoven

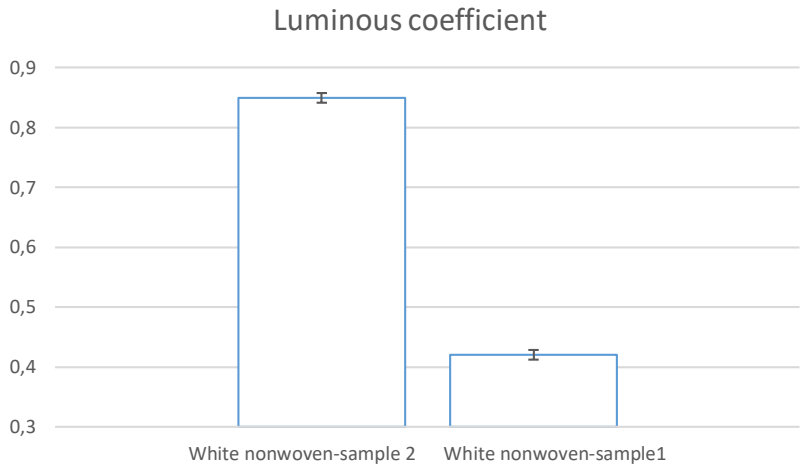

Fig. 6. Luminance coefficient β for samples 1 and 2 on a white nonwoven

on a blue background, and sample 2 - with a solid star print pattern on a white background.

The samples were conditioned under the following conditions:
– irradiation with artificial light (fluoreescent lamps), with an intensity at the sample surface of approx. 500 lx for 15 min.,
– in complete darkness for 60 min.

Photographs of the irradiated and non-irradiated samples were taken directly after conditioning under relatively low light conditions (approx. 50 lx). The camera exposure time and aperture settings were the same for both samples.

4.2.1. RGB value comparison for sample 1

Figures 7 and 8 show photographs of the surface of sample 1 after conditioning (with and without irradiation). Both photographs were taken with the same camera settings (exposure time 3.2 s, aperture *f*/5.6). Since the pattern printed on sample 1 represents an open star, the RGB values were read from the outline of the shape.

Even a subjective visual evaluation of the images (photographs and histograms) shown in Figures 7 and 8 indicates that the pattern became more conspicuous following irradiation. This is corroborated by the RGB values determined for the irradiated and non-irradiated patterns (star outlines). Table 9 contains the RGB values measured, while Figure 9 presents a bar graph of mean RGB values for the irradiated and non-irradiated material.

The measurements show that the RGB values for the irradiated material were much higher than those for the non-irradiated one, with the largest differences found for the green colour (41.9±3.6 vs. 78.7±5.9). Statistically significant differences were found only for the red colour; the differences for blue were relatively small (38%).

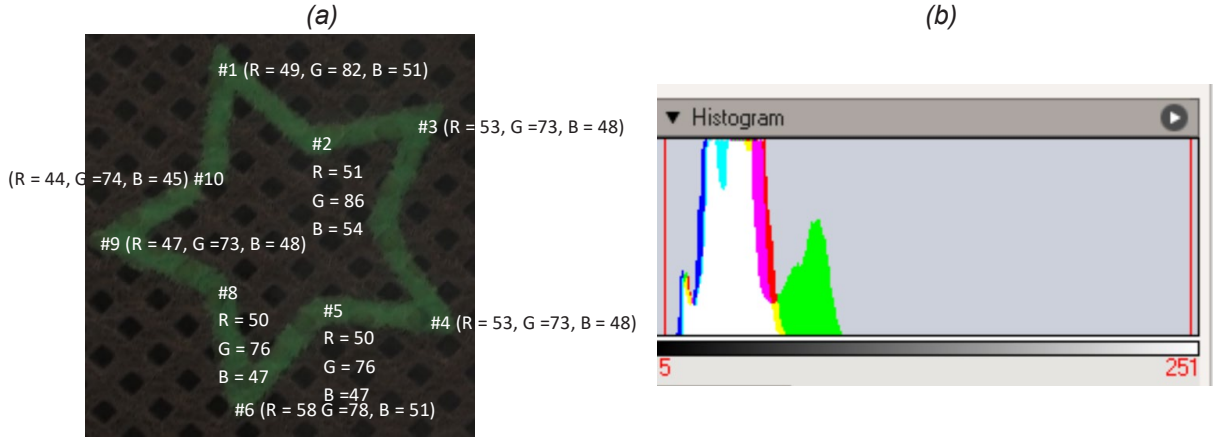

Figure 7. Irradiated sample 1: (a) photograph of the star pattern; (b) histogram

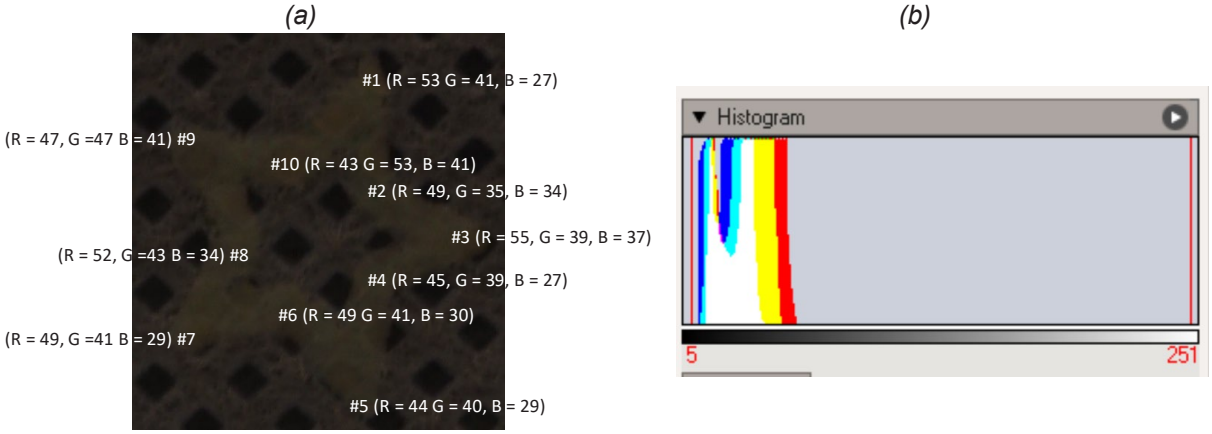

Figure 8. Non-irradiated sample 1: (a) photograph of the star pattern; (b) histogram

Measurement No.	Irradiated sample			Non-irradiated sample		
	R	G	B	R	G	B
1	49	82	51	48	39	26
2	51	86	54	49	45	34
3	53	73	48	55	49	37
4	53	77	53	45	39	27
5	50	76	47	44	40	29
6	58	78	51	49	41	30
7	50	91	50	49	41	29
8	50	76	47	52	43	34
9	48	74	47	47	41	29
10	48	74	45	53	41	27
Mean	**51**	**78.7**	**49.3**	**49.1**	**41.9**	**30.2**
Standard deviation	**3.0**	**5.9**	**2.9**	**3.4**	**3.1**	**3.6**

Table 9. RGB values measured for the outline of the open star pattern

4.2.2. Comparison of RGB values for sample 2

Figures 10 and 11 show images of irradiated and non-irradiated samples. The points at which RGB values were measured are marked in the photographs. Both photographs were taken at the same camera settings (exposure time 3.2 s; f/5.6). As the pattern printed on sample 2 consists of filled geometric shapes (solid stars), RGB values were read from randomly selected prints (stars).

RGB values measured are given in Table 10, while Figure 12 presents a bar graph of mean RGB values for irradiated and non-irradiated samples.

Analysis of the results indicates that sample 2 (solid stars on a white background) is more conspicuous following illumination (irradiation). The mean values for the green colour were the highest at 127.1 ± 6.7, followed by blue at 73.6 ± 5.4; while the lowest RGB values were found for red at 53 ± 6.8.

5. Conclusions

The paper presents the possibilities of assessing the optical properties - visibility of anti-smog models of half-masks with

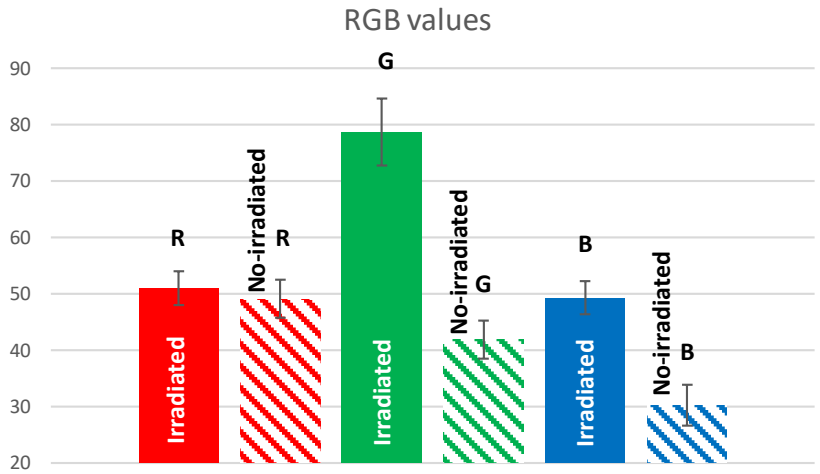

Figure 9. Mean RGB values measured for the open star pattern outline

new functionalisation.. Half-mask outer layers were printed with phosphorescent dye, increasing their visibility under smog conditions. It was also shown that the two patterns designed did not affect the deterioration of the filtration properties. Two colours of the background material of the outer and inner layers and two types of pattern: solid and open stars were used.

Two methods for objective evaluation of optical properties were proposed based on the reflectance coefficient, chromaticity coordinate determination using a reflectometer, and luminance determination using digital image analysis.

a) *(b)*

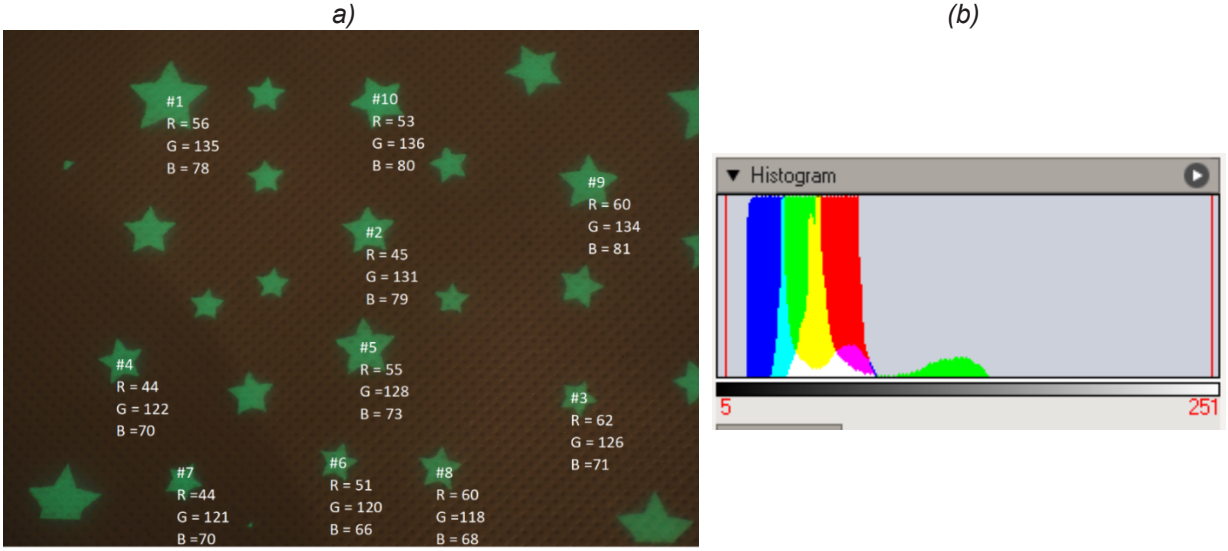

Fig. 10. Irradiated sample 2: (a) photograph of the star pattern; (b) histogram

(a) *(b)*

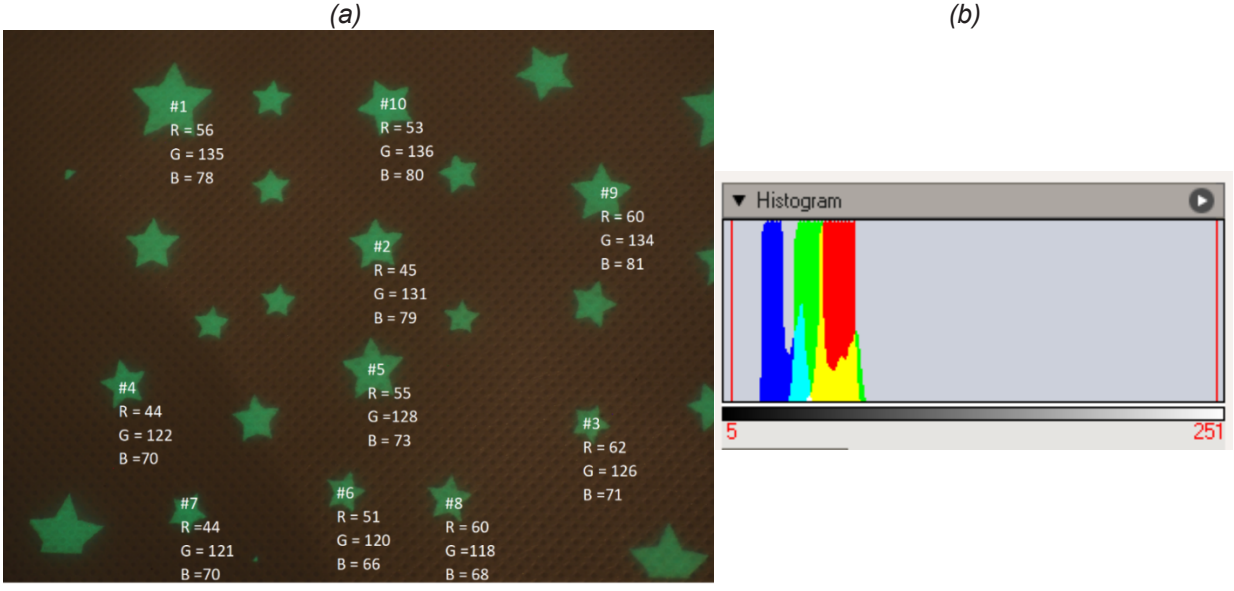

Fig. 11. Non-irradiated sample 2: (a) photograph of the star pattern; (b) histogram.

Measurement No.	Irradiated sample			Non-irradiated sample		
	R	G	B	R	G	B
1	56	135	78	56	71	49
2	45	131	79	58	73	44
3	62	126	71	58	71	43
4	44	122	70	52	64	40
5	55	128	73	55	69	43
6	51	120	66	57	70	42
7	44	121	70	50	62	38
8	60	118	68	54	64	49
9	60	134	81	56	71	42
10	53	136	80	58	41	45
Mean	**53**	**127.1**	**73.6**	**55.4**	**64.6**	**43.5**
Standard deviation	**6.8**	**6.7**	**5.4**	**2.7**	**9.4**	**3.5**

Table 10. RGB values measured for the solid star pattern

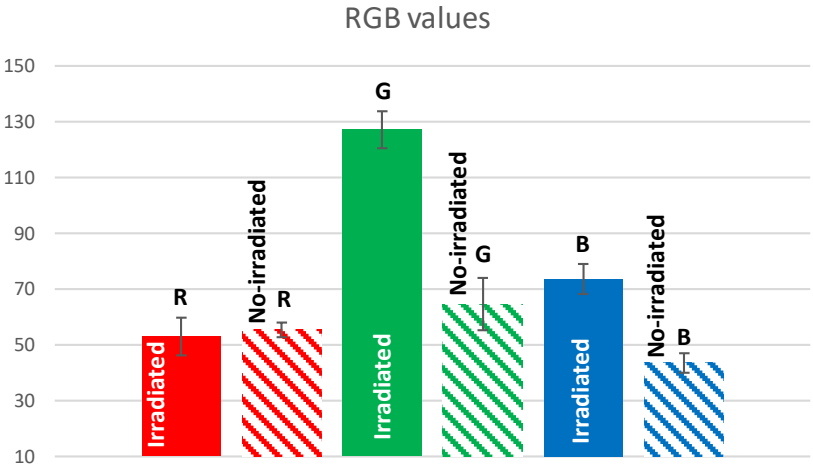

Fig. 12. Mean RGB values measured for the solid star pattern surface

The analysis of RGB values from digital images is useful for assessing the phenomenon of phosphorescence - increasing visibility after lighting (irradiation)

Reflectance results indicate that under dark conditions better visibility can be obtained using white material with a print pattern containing solid shapes. However, it should be remembered that the more phosphorescent print on the surface of the material, the more the air flow resistance may increase. Therefore, a compromise has to be found between good visibility and air flow resistance. This conclusion is very useful for face mask designers.

Further development of the method of determining luminance from digital images proposed may constitute an element of laboratory evaluation of the potential visibility of materials with phosphorescent patterns intended for face masks. Anti-smog and other face masks with phosphorescent print on their outer layers are conspicuous after dark. The research will be continued to evaluate the properties that determine face mask visibility under real-life conditions.

Acknowledgements

The publication is based on the results of Phase V of the multi-year program "Improvement of occupational safety and working conditions," financed in the years 2020–2022 in the area of research and development by the Ministry of Science and Higher Education and the National Center for Research and Development. Program coordinator – the Central Institute for Labour Protection–National Research Institute.

References

1. The online version of the PWN Polish dictionary, https://sjp.pwn.pl/poradnia/haslo/widzialnosc-czy-widocznosc;13297.html, (in Polish) accessed November 18, 2021
2. Head, Eye, and Face Personal Protective Equipment, CRC Press, Taylor & Francis Group, Boca Raton 2021, ed. K. Majchrzycka
3. Szkudlarek J. Snycerski M., Owczarek G.; Proposal of Objective Assesment of the Phenomenon of Light Passage through Blackout Fabrics; FIBRES & TEXTILES in Eastern Europe, Vol.: 25, Issue: 4, pp: 50-58
4. Pościk A., Łężak K. Warning clothing - requirements and assessment of materials, Work Safety. Science and Practice, 6/2002, pp. 20-23
5. REGULATION (EU) 2016/425 OF THE EUROPEAN PARLIAMENT AND OF THE COUNCIL of 9 March 2016 on personal protective equipment and repealing Council Directive 89/686/EEC
6. Mingxing Zhang, Junchang Chen, Maojiang Zhang, Rong Li, Minglei Wang, Long Qiu, Mengjia Yuan, Xinxin Feng, Zhe Xing, Jiangtao Hu, and

Guozhong Wu, Radiation-Induced In Situ-Printed Nonconjugated Fluorescent Nonwoven Fabric with Superior Fluorescent Properties, ACS Appl. Mater. Interfaces, 2020, 12, 43, 49258–49264, doi: 10.1021/acsami.0c16657

7. Sweta Narayanan Iyer , Nemeshwaree Behary, Vincent Nierstrasz , Jinping Guan;Glow-in-the-Dark Patterned PET Nonwoven Using Air-Atmospheric Plasma Treatment and Vitamin B2-Derivative (FMN), Sensors 2020, 20, 6816; doi:10.3390/s20236816
8. Mingxing Zhang, Junchang Chen, Minglei Wang, Mengjia Yuan, Rong Li, Xinxin Feng, Yulong He, Xuanzhi Mao, Yulong Li, Zhi Xiong, Zhe Xing, Jiangtao Hu, and Guozhong Wu, Pyrene-Based Nonwoven Fabric with Tunable Fluorescence Properties by Employing the Aggregation-Caused Quenching Effect , ACS Appl. Mater. Interfaces 2021, 13, 7, 9036–9042
9. Brochocka, M. Pośniak, J. Skowroń, Filtering half masks for protection against smog (in Polish), Work Safety. Science and Practice, 2018, 9, 564, 8-13
10. Saraswati Anindita Rizki, Andree Kurniawan, Efficacy of Cloth Face Mask in Reducing COVID-19 Transmis s ion: A Literature Review, National Public Health Journal, 2020; Special Issue 1: 43-48
11. William G. Lindsley, John D. Noti, Francoise M. Blachere, Jonathan V. Szalajda, and Donald H. Beezhold, Efficacy of Face Shields Against Cough Aerosol Droplets from a Cough Simulator, Journal of Occupational and Environmental Hygiene, 11: 509–518, doi: 10.1080/15459624.2013.877591
12. Zou, L. Ruan F, Huang M, et al. SARS-CoV-2 Viral Load in Upper Respiratory Specimens of Infected Patients. N Engl J Med 2020; 382(12):1177–1179. doi: 10.1056/NEJMc2001737
13. https://ourworldindata.org/coronavirus accessed November 18, 2021
14. EN ISO 20471: 2013 / A1: 2016 High Visibility Clothing - Test methods and requirements (in Polish), Warsaw, PKN, 2018
15. https://cie.co.at/news/cie-tc-3-59-new-tc-integration-daylight-and-electric-lighting-photometric-colorimetric-and, accessed November 18, 2021